Cancer Chemotherapy and Pharmacology (2019) 84:1073–1087
https://doi.org/10.1007/s00280-019-03941-z

ORIGINAL ARTICLE

Development of a physiologically based pharmacokinetic model for intravenous lenalidomide in mice

Jim H. Hughes[1] · Richard N. Upton[1] · Stephanie E. Reuter[1] · Darlene M. Rozewski[2,3] · Mitch A. Phelps[2,3] · David J. R. Foster[1]

Received: 21 March 2019 / Accepted: 23 August 2019 / Published online: 6 September 2019

Abstract

Purpose Lenalidomide is used widely in B-cell malignancies for its immunomodulatory activity. It is primarily eliminated via the kidneys, with a significant proportion of renal elimination attributed to active processes. Lenalidomide is a weak substrate of P-glycoprotein (P-gp), though it is unclear whether P-gp is solely responsible for lenalidomide transport. This study aimed to determine whether the current knowledge of lenalidomide was sufficient to describe the pharmacokinetics of lenalidomide in multiple tissues.

Methods A physiologically based pharmacokinetic model was developed using the Open Systems Pharmacology Suite to explore the pharmacokinetics of lenalidomide in a variety of tissues. Data were available for mice dosed intravenously at 0.5, 1.5, 5, and 10 mg/kg, with concentrations measured in plasma, brain, heart, kidney, liver, lung, muscle, and spleen. P-gp expression and activity were sourced from the literature.

Results The model predictions in plasma, liver, and lung were representative of the observed data (median prediction error 13%, − 10%, and 30%, respectively, with 90% confidence intervals including zero), while other tissue predictions showed sufficient similarity to the observed data. Contrary to the data, model predictions for the brain showed no drug reaching brain tissue when P-gp was expressed at the blood–brain barrier. The data were better described by basolateral transporters at the intracellular wall. Local sensitivity analysis showed that transporter activity was the most sensitive parameter in these models for exposure.

Conclusion As P-gp transport at the blood–brain barrier did not explain the observed brain concentrations alone, there may be other transporters involved in lenalidomide disposition.

Keywords Distribution · Lenalidomide · Mouse · Physiologically based pharmacokinetics · Transporters

Introduction

The oral immunomodulatory drug, lenalidomide, has become extensively used in multiple myeloma, myelodysplastic syndromes, and mantle cell lymphoma [1]. This is largely attributed to the medication's mechanism of action being well suited for the treatment of B-cell malignancies. By binding to cereblon, lenalidomide causes antiproliferative and antiangiogenic effects via downstream signalling [2, 3] while also increasing activity of immune effector cells [4, 5]. While lenalidomide's mechanism of action is theoretically suitable for treating B-cell malignancies, it also has shown promise in the treatment of patients with central nervous system tumours [6–9]. The use of lenalidomide is complicated in chronic lymphocytic leukaemia (CLL), where the disease-specific side effect of tumour flare may

Electronic supplementary material The online version of this article (https://doi.org/10.1007/s00280-019-03941-z) contains supplementary material, which is available to authorized users.

✉ Jim H. Hughes
jim.hughes@mymail.unisa.edu.au

[1] School of Pharmacy and Medical Sciences, University of South Australia, North Terrace, Adelaide 5001, Australia

[2] Comprehensive Cancer Center, The Ohio State University, Columbus, OH, USA

[3] Division of Pharmaceutics, College of Pharmacy, The Ohio State University, Columbus, OH, USA

occur. This is characterised by an increase in circulating CLL B cells and the potential for life-threatening tumour lysis syndrome [10]. As a result, lenalidomide is currently not recommended in patients with CLL outside of controlled clinical trials.

Lenalidomide elicits its effects in both the plasma and tissues, where cancer cells aggregate. In B-cell malignancies, these tissues are typically the spleen, bone, and lymph nodes of the patient [11–13]. In these tissues, tumour cells are able to interact with a microenvironment that becomes a sanctuary for the cancerous cells. By inhibiting cytokine production, upregulating tumour suppressor genes, and activating cell apoptosis pathways, lenalidomide is able to increase the tumoricidal activity of the tumour cells [14–16]. The main grade 3/4 toxicities of lenalidomide are fatigue, neutropenia, and thrombocytopenia [17–20]. Plasma concentrations of lenalidomide correlate with the occurrence and severity of haematological toxicities, with the area under the concentration–time curve (AUC) being a significant predictor for thrombocytopenia and being associated with neutropenia [21]. No significant relationship has been established between maximum concentrations (C_{max}) and toxicity [22].

The basic pharmacokinetics of lenalidomide are well covered in the literature. The molecule distributes moderately into tissues and is cleared quickly, having an apparent volume of distribution of 75–125 L and an apparent clearance of 12 L/h in young healthy volunteers. In addition, it binds moderately with plasma proteins, with protein binding ranging from 22.7 to 29.2% [23]. Lenalidomide has a high bioavailability (> 90%) and is given orally once daily [24], with a typical cycle involving 21 days of dosing with 7 days off [18–20].

The main excretion pathway for lenalidomide is the kidneys, with unchanged lenalidomide in the urine accounting for 84% of the dose within 24 h [25]. The renal clearance of lenalidomide exceeds glomerular filtration rate by approximately twofold, suggesting that renal secretion occurs and is responsible for at least 50% of renal elimination. This active transport appears to be due, at least in part, to lenalidomide being a weak substrate of P-glycoprotein (P-gp) [26]. No other renal transporters have been identified that transport lenalidomide. Hydrolysis and metabolism, though very minor, are thought to comprise the remaining proportion of lenalidomide elimination, with metabolism occurring through hydroxylation and acetylation [27].

The pharmacokinetics of lenalidomide have been extensively studied in plasma. Multiple population pharmacokinetic models exist in literature that describe the inter-individual variability of lenalidomide, with renal function explaining some of the variability observed in lenalidomide clearance [28, 29]. Drug kinetics in other tissues are lacking in comparison. Brain kinetics have been studied, with the brain exposure of lenalidomide found to be consistently lower than its chemical analogue thalidomide. While thalidomide often has concentrations in cerebrospinal fluid that are ~ 50% of plasma, lenalidomide has a relative exposure to plasma of ~ 10% in non-human primate and human brains [30, 31]. Previous work by Rozewski et al. found that brain tissue concentrations in mice are 0.9–2.3% of plasma concentrations [32]. This work also identified relatively high lenalidomide exposure in the spleen when normalising AUC to organ perfusion rate.

Having knowledge around tissue pharmacokinetics, particularly in tissues where lenalidomide has tumoricidal effects or causes toxicity, could provide further insight into the tissue-specific pharmacodynamics of the drug. Development of PBPK models can be an effective strategy for characterising and predicting tissue-specific exposures of drug and linking these exposures to local pharmacodynamic effects. This is done by representing drug kinetics in one or more organs, and these organ sub-models are subsequently connected to describe the kinetics of the "whole body" [33]. The objective of this study was to determine whether the current knowledge of lenalidomide could sufficiently describe its pharmacokinetics in multiple tissues. This would be achieved by developing a PBPK model using this knowledge and evaluating its ability to describe concentrations in the plasma, brain, kidney, heart, lung, spleen, liver, and muscle. This manuscript is part of a larger body of work investigating the effectiveness of the extrapolation of lenalidomide kinetics in mice to other species, including humans, to help define the utility of PBPK modelling for this class of drugs.

Materials and methods

Preclinical data set

The data used for development of the model were collected in a preclinical study described previously [32]. The study involved dosing ICR (Institute of Cancer Research) mice at 8–10 weeks of age with lenalidomide. Mice were given lenalidomide by intravenous bolus injection and were dosed by body weight at 0.5, 1.5, 5, and 10 mg/kg. Animals were euthanised and samples collected at the times 2, 10, 20, 45, 60, 90, 180, 300, and 480 min, with 4–5 mice used per timepoint. Tissue samples included plasma, liver, lung, heart, spleen, kidney, hind limb muscle, and brain. Plasma concentrations were determined using established LC–MS/MS methods [34]. Care for the animals and experiments performed upon animals were approved and compliant with the Institutional Animal Care and Use Committee guidelines.

Software and model specification

PBPK modelling was conducted using the open source software PK-Sim® and MoBi® from the Open Systems Pharmacology Suite (Bayer) version 7.2.1 [35]. PK-Sim® parameter optimisation was performed using the software's in-built Monte Carlo algorithm. During optimisation, observed data below the LLOQ were handled using the M6 method as outlined by Beal [36]. Briefly, the first data point below the LLOQ was replaced with a value of half the LLOQ, with the later timepoints being removed from the analysis. Processing of data for input into PBPK software and creation of figures from software output was performed using R v3.3.3 [37].

The structure used in model development was based on a mean individual, using the default PK-Sim mouse model scaled to a weight of 30 g (Fig. 1). A summary of the differential equations used can be found in Supplemental Material 1. The physicochemical properties of lenalidomide were sourced from DrugBank [38, 39]. Potential physiological processes were specified before model development. These processes included: renal elimination including secretion, transport via P-gp transporters or other unspecified transporters, and non-renal elimination. For parameters such as fraction unbound, where no literature values existed for mice, human values were used in their place [23, 26, 27]. The active transporter responsible for secretion was defined using expression data of the *Abcb1a* and *Abcb1b* genes in mice [40] responsible for production of transporters analogous to P-gp in humans (Supplementary Table 1). The transporters were located basolaterally in most tissues (Fig. 1c) while being in the apical membrane of the kidney to represent renal secretion. Liver P-gp transporters were located basolaterally, to prevent apical transport of the drug to the gallbladder.

Michaelis–Menten-type kinetics were used to describe transporter kinetics, with parameters sourced from the literature [26]. The V_{max} parameter could not be used, as it was provided in nmol/m^2/min with no protein concentration provided for the P-gp in the test environment. As a result, only the in vitro K_m value (802 µmol/L) could be used in the model. V_{max} for 1 µmol/L of P-gp transporters was estimated during model development, thus making V_{max} equal to the

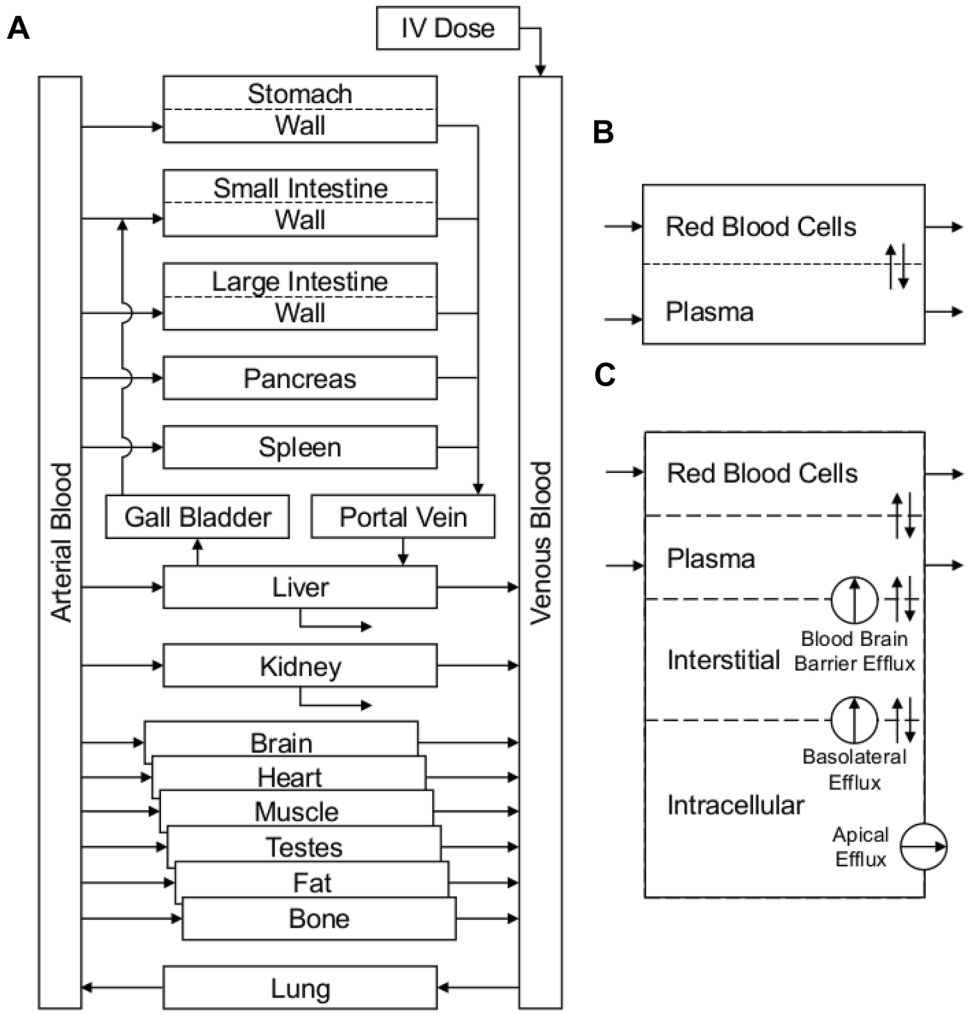

Fig. 1 Schematic of the model components of the base PK-Sim® mouse model. The physiologically based pharmacokinetic model structure is shown including **a** tissue compartments that make up the whole body, **b** compartments that make up each blood vessel and **c** the compartments that make up each tissue

transporter rate constant, k_{cat}. Table 1 presents the parameters used to develop the model, excluding the parameters provided as a part of the base PK-Sim® model.

The non-renal component of lenalidomide's elimination was modelled using first-order kinetics, which could represent Michaelis–Menten kinetics in the linear portion of the curve (well below K_m). As there was no way to differentiate hydrolysis from metabolism due to the lack of metabolism kinetic data, they were represented as a single process during model development. The combined non-renal elimination was represented by the relatively slow rate of elimination that is known to occur directly in plasma (8 h half-life) [27]. The elimination rate constant of drug loss in the plasma was estimated during model development. In addition, the elimination rate constant in each tissue was estimated to be relatively higher or lower than the plasma elimination rate constant.

Model development

The model was developed in a stepwise fashion. This began with modelling simple processes to describe whole-body pharmacokinetics, which could then be evaluated to determine which aspects of the model required increased complexity. The first model used a simple first-order process to move drug from the kidney plasma to the urine, to determine if predictions of tissue concentrations could be made using plasma clearance values from the literature. The plasma clearance implemented in the model was sourced from earlier analysis of the observed plasma concentrations [32]. The renal elimination was then split into two processes, glomerular filtration and secretion from kidney cells. Glomerular filtration was assumed to be unimpaired. Secretion was implemented using the gene expression data for P-gp transporters defined during model specification, modelling both the renal secretion in the kidney and the efflux by P-gp in the tissues. Various P-gp transporter configurations were tested in the brain, specifically changing the location (blood–brain barrier vs. basolateral as defined in Fig. 1c) and the level of expression in the tissue.

The addition of non-renal elimination was also evaluated during model development. The elimination rate constant per 1 µmol/L for the non-renal elimination was determined by isolating the plasma compartment of the venous blood (Fig. 1b). The PK-Sim® model and parameters were imported into MoBi® to facilitate changes to the model structure and development of the isolated plasma model. The elimination rate constant was estimated such

Table 1 Final parameter values used in lenalidomide PBPK models

Parameter	Value (95% confidence intervals)
Partition coefficients	Calculated by PK-Sim®[a]
Cellular permeability	Calculated by PK-Sim®[a]
Physicochemical properties[b]	
Molecular weight	259.26 g/mol
Lipophilicity (logP)	−0.4
Solubility (at pH 7)	2330 mg/L
Acidic pka	10.75
Basic pka	2.77
Fraction unbound[c]	0.7
Glomerular filtration rate fraction	1.00
Abcb1a transporter	
Transporter concentration	1.00 µmol/L
Michaelis constant (K_m)[d]	802 µmol/L
Hydrolysis	
Elimination rate constant[e]	0.00206 min^{-1}
Estimated parameters–final transport model	
Maximum rate of reaction (V_{max})	29800 (22,800–36,900) µmol/L/min
Estimated parameters–final hydrolysis model	
Maximum rate of reaction (V_{max})	29,100 (22,600–35,600) µmol/L/min
Relative extent of hydrolysis (Brain)	7.40 (2.00–12.8)

[a]Partition coefficients calculated as specified by Willmann et al. [46]

[b]Physicochemical properties sourced from Drugbank [38]

[c]Human fraction unbound sourced from Revlimid® product information [23]

[d]K_m value for human P-gp sourced from Tong et al. [26]

[e]Estimated using the half-life of lenalidomide in plasma as an initial estimate

that the half-life of the drug in the plasma was 8 h. Using this elimination rate constant, different whole-body models were evaluated. These models differed in the extent and location of the non-renal elimination. Non-renal elimination was tested in all tissues, with the extent of the elimination being estimated relative to its activity in plasma.

The suitability of the model processes and parameters was determined by comparing predictions from simulations with the mean pooled preclinical data for each dose and tissue. This comparison was undertaken assuming a proportional error model. For tissues where the observed data were not represented well by the model predictions, a single-tissue model was created for further refinement of the model. This allowed the rate of drug flowing into the tissue to be fixed, ensuring that concentrations moving into the tissue were representative of the observed plasma concentrations. By providing an accurate description of the concentrations flowing into the tissue, misspecification of tissue parameters had no influence upon the evaluation of tissue-specific processes for both renal and non-renal elimination. These individual tissue models were used to adjust elimination and protein expression parameters to obtain a better description of observed data in specific tissues.

For detailed analysis of data from single organs, single-tissue models were created by importing PK-Sim® simulations into MoBi® and altering the compartments, so that only arterial blood, venous blood, and the tissue of interest were present. While other tissue compartments were removed from the model, all model parameters provided by PK-Sim® remained the same. As the model was not recirculatory, a forcing function was used to control the amount of drug that entered the tissue, and the kinetics of the drug in other organs and plasma could be ignored. Parameter estimates were determined for a sum of exponential equation that represents the venous blood concentrations. These estimated values were set as global parameters within MoBi® and used to provide arterial concentrations as the forcing function. During development of single-tissue models, parameter values for elimination pathways were empirically approximated.

Once the model sufficiently predicted the concentration profiles described by the preclinical data, it was optimised to identify parameter estimates that provided better predictions of observed tissue concentrations. Single-tissue model parameters were then used to update the whole-body model in PK-Sim®. These updated parameters underwent further optimisation to ensure parameter values from the single-tissue models were appropriate for the whole-body model. Parameters were optimised individually to avoid problems with identifiability. Final models were assessed and compared using a log-likelihood function, goodness-of-fit plots, and physiological plausibility.

Sensitivity analysis

To calculate the sensitivity of pharmacokinetic metrics ($AUC_{0\text{-inf}}$, C_{max}) to changes in model parameters, a local sensitivity analysis was conducted on the model that best represented the data. This involved the calculation of a sensitivity index (S) that shows the relative change in the pharmacokinetic metric when a parameter is altered. Model simulations, where parameter i was perturbed from its original value (x_i) by a variation factor (k), were completed. The difference between pharmacokinetic metric j in the new simulation (f_j) and the old simulation was subsequently calculated. As demonstrated in Eq. 1, the sensitivity of a pharmacokinetic metric was defined as the ratio of the relative change in the metric ($\Delta f_j / f_j$) and the relative variation of the model parameter ($\Delta p_i / p_i$). Model parameters were perturbed by n different variation factors ($n = 4$, $k = 1/1.1, 1/1.05, 1.05, 1.1$). The average sensitivity was calculated from the sensitivities determined from each variation factor:

$$S_{i,j} = \frac{\sum_k^n \frac{\Delta_k f_j}{\Delta_k p_i} \cdot \frac{p_i}{f_j}}{n} \quad (1)$$

where $S_{i,j}$ was the sensitivity index value of metric j to changes in parameter i, f_j was the value of metric j, and p_i was the parameter value for parameter i.

Results

Preclinical data set

The pharmacokinetic data obtained from the previous preclinical study in 170 mice were stratified into four different dose groups. Each mouse provided concentration samples for eight tissues, with 4–5 mice providing the concentrations for one timepoint [32]. Of the 1360 concentration samples, 14.3% were below the LLOQ. Half of these missing values were a result of all brain concentrations from the 0.5 and 1.5 mg/kg dose levels being below the LLOQ. The LLOQ values for: plasma, brain, muscle, and heart tissue were 0.3 nM; lung tissue was 1 nM; liver, spleen, and kidney tissue were 10 nM.

Early model development

When using the literature value for total clearance in mice as a first-order process representing renal clearance, plasma concentrations were predicted well by the model. Due to the simplicity of its description of physiological processes, the model failed to describe concentrations in the heart,

muscle, kidney, and brain. The brain concentrations had the worst predictions, with C_{max} of lenalidomide in the brain predicted to be 1000-fold less than concentrations in plasma. Predictions also showed that lenalidomide was retained in the brain (particularly in the intracellular space), declining at an imperceptible rate despite plasma concentrations falling more than 1000-fold over the same period (Fig. 2a).

This was contrary to the observed data, which contained concentrations typically 100-fold less than plasma and was cleared from the tissue at a similar rate to plasma, producing a much lower AUC. When using glomerular filtration and P-gp mediated transport in all tissues governed by gene expression data from either *Abcb1a* or *Abcb1b*, the model predicted that no drug would enter the brain (Fig. 2b). The heart, muscle and kidney were also poorly predicted. As a result, single-tissue models were developed for the brain, heart, muscle and kidney to estimate P-gp abundance in these tissues.

Single-tissue models

A single-tissue model was developed for the brain. This resulted in the development of two competing models that provided an adequate representation of brain pharmacokinetics. Both models were based on an original brain model, where P-gp transporters were located in the blood–brain barrier. Given that cytochrome P450 enzymes are present in the brain [41], it was hypothesised that reactions responsible for lenalidomide's non-renal elimination (e.g., degradation, acetylation, and hydroxylation) may also occur in the brain. Because of this hypothesis, P-gp expression was removed from the brain, and drug metabolism was added in its place to create the first model. This resulted in improvements to the objective function and goodness-of-fit plots, while AUC (74% of observed AUC) and C_{max} (16% of observed C_{max}) showed modest changes when compared to predictions using no P-gp expression or hydrolysis in the brain (142% and 15% of observed value, respectively). The addition of drug metabolism specifically prevented retention of lenalidomide in the brain. The best predictions were achieved when metabolic activity in the brain was 7.4 times larger than in plasma.

The second model removed the P-gp transporters from the blood–brain barrier and included unspecified basolateral transporters intracellularly, which provided similar estimates of C_{max} (14% of observed) and poorer estimates of AUC

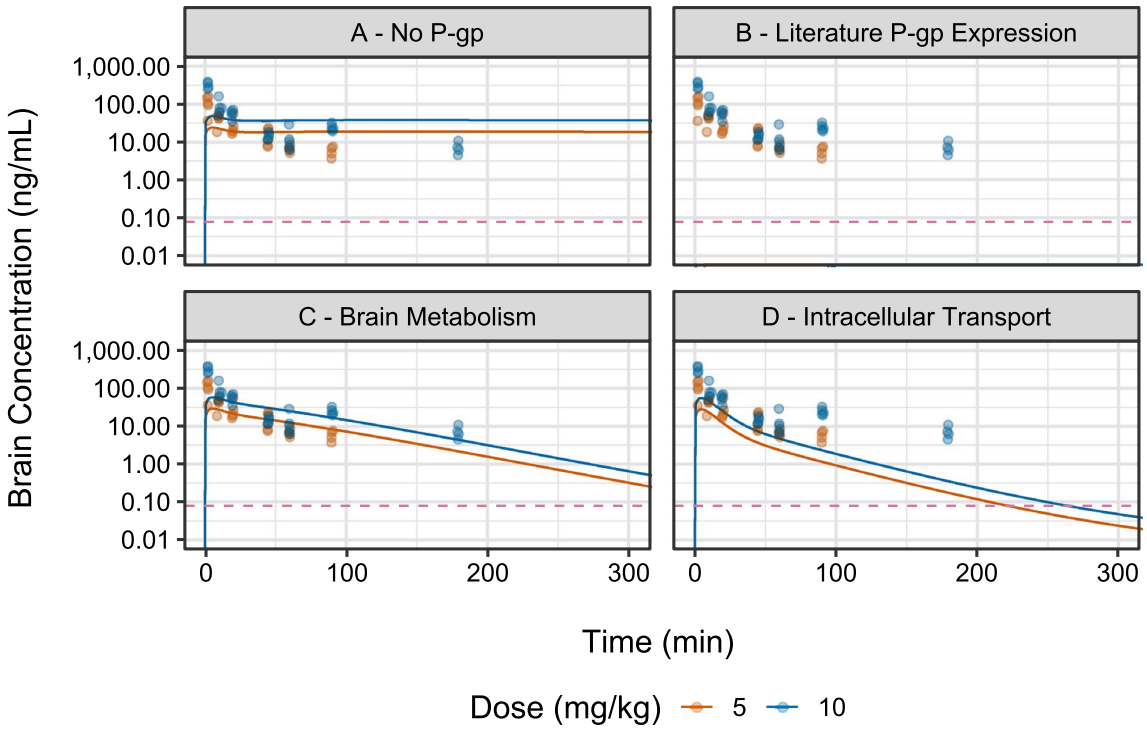

Fig. 2 Lenalidomide concentration–time profiles in brain tissue for different PK-Sim® models. The dots represent observed data from the preclinical data set. The lines represent the predicted concentrations. The colours of the lines and dots correspond to the dosages in the legend. The dashed line represents the lower limit of quantification. The model for each pane are **a** no P-gp expression in the brain, **b** P-gp expression in the brain according to Yue et al. (lack of apparent curve due to predictions being effectively zero), **c** brain elimination with no P-gp expression in the brain (best objective function), and **d** unspecified transport located basolaterally at the intracellular wall with no P-gp expression in the brain

(31.3% of observed) as compared to the values above. This decreased the entry of lenalidomide into the intracellular compartment in the brain, counteracting the retention in this compartment observed in the original brain model. The predictions underestimated the observed brain tissue concentrations and were inferior to the predictions by the blood–brain barrier model with drug elimination in the brain.

Single-tissue models were also developed for the heart, kidney, and muscle. Error associated with predictions for the heart and kidney were reduced (1.91–1.80 and 1.29–1.02 reduction in median proportional prediction error, respectively) through adjusting P-gp expression, using the *Abcb1a* gene expression as a baseline. The estimation of parameters that reduced the prediction error in the muscle tissue was difficult due to the observed concentrations not increasing with doses of lenalidomide above 1.5 mg/kg. This non-linearity in the distribution of lenalidomide to muscle could not be explained through adjusting P-gp expression or non-renal elimination. In the whole-body model, changes in P-gp activity in muscle resulted in poor predictions in other tissues, due to a dramatic shift of drug from the high-volume muscle (30% of total volume) into other tissues. It was concluded that the non-linearity seen in the observed muscle tissue data could not be reasonably represented with the current knowledge of lenalidomide in the literature. As a result, only parameter changes from heart, kidney, and brain single-tissue models were incorporated into the whole-body model.

Development of final model

Based on the results of early modelling in single-tissue models, two hypotheses were tested to improve the model's description of lenalidomide pharmacokinetics. These hypotheses were based on the two single-tissue brain models developed in early modelling. The first hypothesis was that non-renal elimination was responsible for the removal of lenalidomide from the brain ("Hydrolysis model"). The second hypothesis was that intracellular efflux transporters were responsible for the removal of lenalidomide from the brain ("Transport model"). Both were modelled with P-gp abundance as determined during single-tissue modelling (Supplementary Table 1) and assumed no significant P-gp transport at the blood–brain barrier. In addition, P-gp transporter expression was removed from intestinal mucosa, as they were not necessary in the context of an intravenous model. Each of these hypotheses were tested alone, but also under the conditions of non-renal elimination occurring in all tissues or in plasma (Table 2).

Hydrolysis model

The best model under this hypothesis consisted of non-renal elimination in the brain only. The addition of non-renal elimination to tissues other than the brain did not improve the objective function and resulted in worsening of diagnostic plots. Non-renal elimination in the brain was estimated to occur at a rate 7.4 times higher than in plasma (Table 1). While this model had the lowest objective function value of all models tested, it was not favoured due to the unlikely physiological assumption that non-renal elimination was occurring to such a great extent localised only in the brain.

Transport model

The model with the lowest objective function using unspecified transporters situated basolaterally at the intracellular wall also included non-renal elimination from the plasma. The non-renal elimination used the values from the literature for in vitro plasma and provided a modest improvement in objective function over modelling the transporters alone (Table 1). As seen with the "Hydrolysis model", modelling non-renal elimination in all tissues resulted in poor

Table 2 Objective function for final tested models in PK-Sim

Model hypothesis 1	Model hypothesis 2	Objective function value[a]	Final model
No P-gp transport at Blood–brain barrier	Hydrolysis occurs only in brain tissue	501,847	No
Basolateral transport at intracellular wall of brain cells	Hydrolysis occurs only in plasma	539,332	Yes
Basolateral transport at intracellular wall of brain cells	No hydrolysis	547,080	No
No P-gp transport at Blood–brain barrier	Hydrolysis occurs only in brain tissue and plasma	582,819	No
Basolateral transport at intracellular wall of brain cells	Hydrolysis occurs in all tissues	637,015	No
No P-gp transport at Blood–brain barrier	No hydrolysis	681,771	No
No P-gp transport at Blood–brain barrier	Hydrolysis occurs in all tissues	750,453	No
P-gp transport at Blood–brain barrier (literature values)	No hydrolysis	NA[b]	No

[a]Objective function value was calculated as AIC and was computed externally from PK-Sim

[b]Due to predictions in the brain being effectively zero the sum of the log-likelihood for brain concentrations exceeded the largest possible floating point value of the computer used for analysis

predictions. As the "Transport model" had the best balance of objective function value, goodness-of-fit, and physiological plausibility, it was chosen as the final model.

Evaluation

Table 1 outlines the final optimised parameters for the best models for both the "Hydrolysis model" and "Transport model". Both models could predict concentrations for most tissues, as shown in Fig. 3, but differed in their predictions of brain concentrations (Fig. 2c, d). At later timepoints, the models performed less favourably for all tissues, where concentrations were closer to the LLOQ. This is also seen in diagnostic plots when comparing observed concentrations to the predicted concentrations, where observed concentrations were higher than predicted concentrations at lower values (Fig. 4). The weighted residuals of the predictions also showed increased error at lower concentrations and later timepoints (Supplementary Figures 1 and 2), but were acceptable at earlier timepoints, where concentrations were not as close to the LLOQ. Table 3 shows the prediction metrics for the model. It shows that plasma, liver, and lung tissue had relatively low prediction error and were able provide accurate estimates of AUC. The heart, kidney, and spleen tissue had poorer performance, but still had 90% confidence intervals that included 0% prediction error. The brain and muscle tissue concentrations were systematically under- and over-predicted, respectively.

Sensitivity analysis

The sensitivity analysis investigated the impact of model parameters on pharmacokinetic metrics $AUC_{0\text{-inf}}$ and C_{max}. It was performed on the more plausible model, using basolateral transporters in the brain and non-renal elimination occurring in plasma only. Figure 5 illustrates the relative changes of these metrics in each tissue for the 10 most influential parameters. The AUC was sensitive to both the activity and expression of P-gp transporters, as well as the physiological parameters of the kidney. The AUC of concentrations in the brain were sensitive to parameters involved with the P-gp transporters and non-renal elimination. It is likely that non-renal elimination parameters would be influential in any tissue, where they are present. C_{max} in the liver and kidney was most affected by P-gp model parameters, with no substantial effects from other estimated parameters.

Discussion

The physiologically based pharmacokinetic models presented described lenalidomide concentrations in mouse plasma and tissues after intravenous administration. The model development process has shown that the current knowledge of lenalidomide pharmacokinetics is insufficient to describe lenalidomide concentrations in the brain. The speculative final model suggests that lenalidomide is relatively unaffected by P-gp-like transporters at the blood–brain barrier, instead suggesting that the presence of unspecified transporters at the cellular wall plays a more important role in the entry of lenalidomide into the brain. Although adequately represented here as a single unspecified efflux transporter at the cellular wall, this may indeed be the net action of several efflux and influx transport processes located at the both blood–brain barrier and/or the cellular wall of brain cells.

The final model accurately described early lenalidomide concentrations in tissues and became less accurate at later timepoints. This may be a result of concentrations at later times being close to the LLOQ, thus being subject to greater random variability or increased censoring. However, it could also represent the distribution of lenalidomide that is not explained when utilising the PK-Sim® mouse model. The prediction of concentrations in the brain tissue was a limitation of the final model, as it was not clearly superior to predictions of other candidate models (Fig. 2), with its selection over those candidate models predominantly determined by its physiological plausibility. Despite these limitations, the model accurately predicted concentrations for plasma, liver, and lung tissue while providing adequate predictions in heart, kidney, and spleen tissue. These conclusions are made based on the performance metrics in Table 3, understanding that the prediction error and root mean squared error were calculating using samples from individual mice, rather than using the naïve mean pooled approach utilised during model development. Thus, the confidence intervals are broadened, as they include inter-animal variability about the population mean characteristics as well as additional residual unexplained variability at each timepoint.

The brain exposure of lenalidomide is an important aspect of the medication's pharmacokinetics, with studies investigating the use of lenalidomide in solid brain tumours [6–9]. The brain sub-model presented herein is speculative, highlighting major unknowns about the pharmacokinetics of lenalidomide in the brain. The slow distribution between the interstitial and intracellular compartments of the base PK-Sim® model suggests that given the physicochemical properties of lenalidomide, it will be retained in the brain at low concentrations.

When implementing P-gp transporters at the blood–brain barrier based on *Abcb1a* gene expression, the model predicts that no drug is able to enter the brain. The local sensitivity analysis shows that pharmacokinetic metrics for exposure are sensitive to transporter activity in the brain (P-gp or otherwise), identifying it as a key aspect of lenalidomide pharmacokinetics. This suggests that there are transporters other

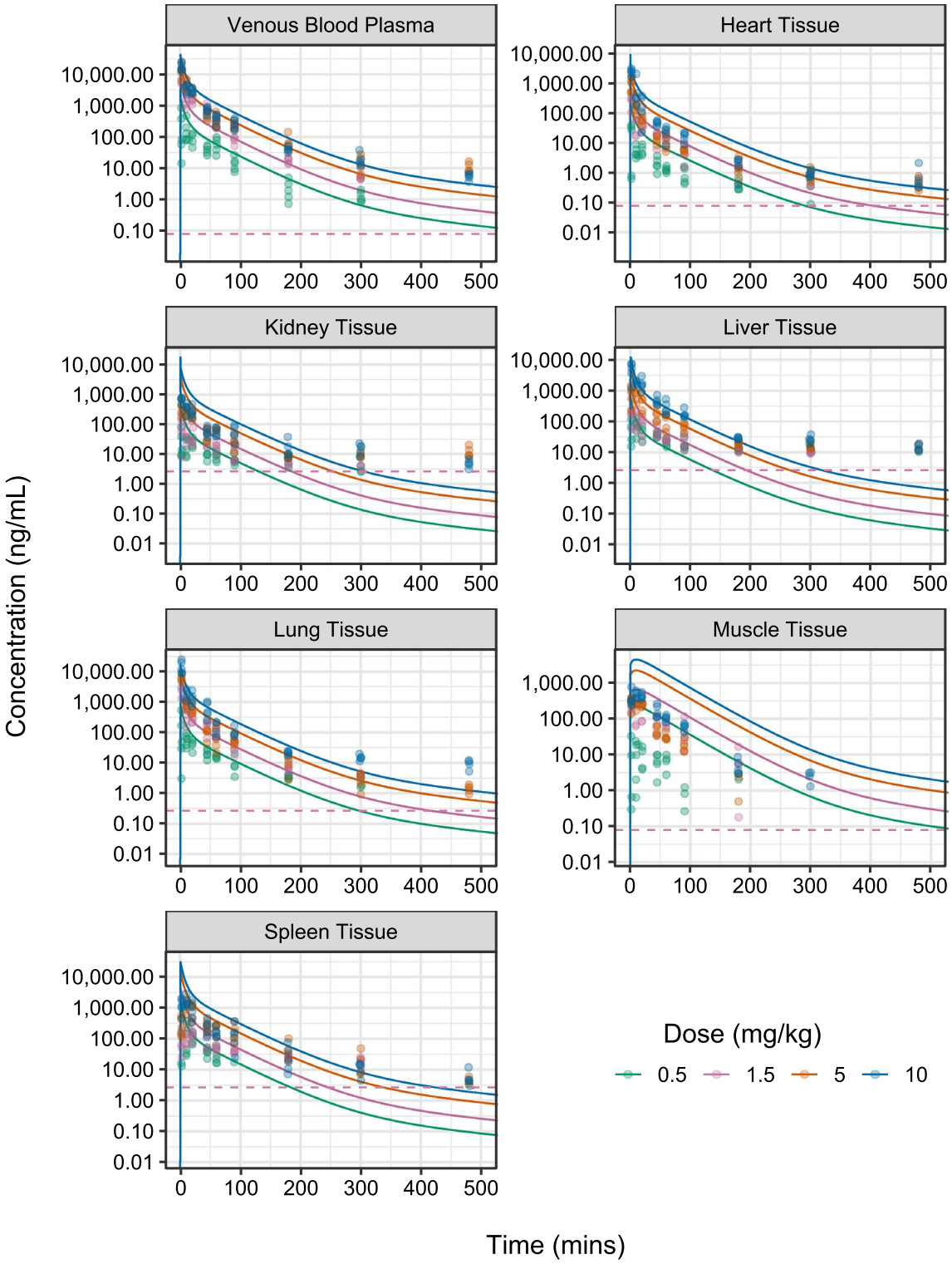

Fig. 3 Lenalidomide concentration–time profiles in multiple tissues. The dots represent observed data from the preclinical data set. The lines represent the predicted concentrations. The colours of the lines and dots correspond to the dosages in the legend. The dashed line represents the lower limit of quantification. Predictions were simulated from the final model using unspecified basolateral transporters in the brain compartment

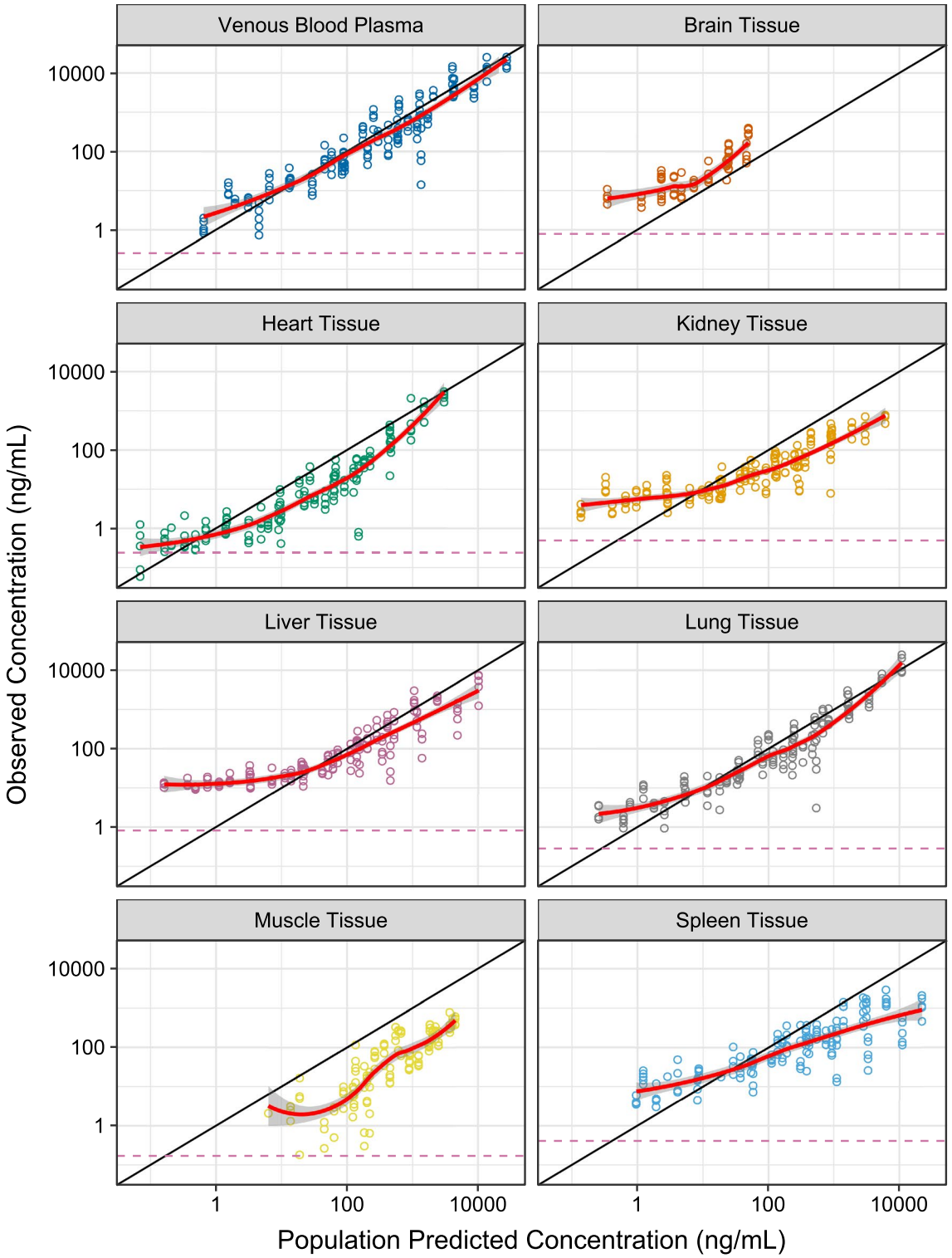

Fig. 4 Model development diagnostic plot providing a comparison between the observed lenalidomide concentrations and the model predictions. Predictions shown are for the model where lenalidomide was affected by unspecified basolateral transport in the brain and non-renal elimination in the plasma. The coloured dots represent the concentrations. The black diagonal line is the line of identity. The red line is a smoothed line (loess) showing the relationship between observed and predicted concentrations, with the grey ribbon representing the 95% confidence intervals

Table 3 Prediction metrics for final model

Tissue	Prediction error (%)		RMSE (%)	AUC_{ratio}	$C_{max\ ratio}$
	Median	90% CI			
Plasma	12.8	−70.3 to 288	770	1.39	0.870
Brain	−62.7	−92.9 to −26.0	67.1	0.313	0.140
Heart	190	−54.2 to 1010	2410	2.71	1.67
Kidney	117	−93.9 to 1090	1020	2.76	4.86
Liver	−9.86	−95.6 to 603	393	1.33	3.45
Lung	29.5	−79.6 to 466	1400	1.31	0.658
Muscle	1070	154 to 8820	7190	11.6	5.05
Spleen	117	−83.9 to 4640	1929	2.85	7.13

Both prediction error and RMSE were calculated as a proportional error of the observed data that has not been naïve mean pooled. AUC_{ratio} was calculated by first dividing the predicted AUC by the AUC of the mean pooled observed data for each dose group. The average was then found for the relative AUC of each dose to produce the AUC_{ratio} value. $C_{max\ ratio}$ was calculated by first dividing the predicted C_{max} by the observed C_{max} for each dose group. The average was then found for the relative C_{max} of each dose to produce the $C_{max\ ratio}$ value

AUC area under the concentration curve, *CI* confidence intervals, C_{max} maximum concentration, *RMSE* root mean squared error

than P-gp that are responsible for transport of lenalidomide. It is possible that P-gp transporters at the blood–brain barrier act as expected, but are outweighed by influx transporter activity. An investigation into the movement of thalidomide across human intestinal Caco-2 monolayers found that the transport of the drug may involve a saturable energy-dependent uptake transporter, such as a nucleoside transporter [42]. Being an analogue of thalidomide, lenalidomide may interact with these nucleoside transporters as well. However, the literature suggests that nucleoside transporters (among numerous other transporters) are unlikely contributors to lenalidomide disposition in the kidney, as lenalidomide was not a substrate for any of those tested [26]. While there are currently no other in vitro or in vivo evidence of transporters that lenalidomide is the substrate for, further investigation of lenalidomide transport in vitro may be worthwhile. To investigate the potential for contribution in other tissues, lenalidomide transport by nucleoside transporters could be investigated in vitro using Caco-2 monolayers, testing for the inhibition of movement across the monolayer using a nucleoside transporter inhibitor such as dipyridamole. Alternatively, an in vivo experiment similar to that conducted by Rozewski et al. could be conducted [32], investigating changes in lenalidomide disposition in mice or rats when a nucleoside transporter inhibitor is administered concurrently. These experiments could generate data to enable the use of more complex models [43], particularly with the availability of Caco-2 experimentation data and observed concentration data in extracellular fluid and cerebrospinal fluid.

The model also raises questions concerning the non-renal elimination of lenalidomide. This component of elimination was modelled as a single source of non-renal elimination using the in vivo half-life of lenalidomide in human plasma [27], representing a combination of hydrolysis, hydroxylation, and acetylation [24]. Mouse data on the proportion of lenalidomide converted to the metabolites of these three processes is required to accurately represent this complexity. During model development, lenalidomide was predicted to distribute out of the brain slowly despite rapidly falling concentrations in the plasma, resulting in retention in brain tissue that was not observed in the data. While the introduction of brain metabolism resolved this, it is unusual for such a large concentration gradient to occur with no discernible change in brain concentrations.

The kinetics defined within PK-Sim® suggest that any drug lipophilic enough to enter the brain and has evidence of the molecule being retained, must undergo metabolism in the brain, or undergo active efflux. There are several pathways that may facilitate the degradation, acetylation, or hydroxylation of lenalidomide in the brain. While spontaneous degradation is most likely, there are several enzymes in the brain that could be responsible for metabolism of lenalidomide. Cytochrome P450 enzymes are present in the brain [41] and are responsible for hydroxylation of two drugs of the same class as lenalidomide: thalidomide and pomalidomide [44]. However, this is unlikely as the enzyme responsible for lenalidomide metabolism given negative results from in vitro experiments [27].

The model with the most accurate predictions also assumes that non-renal elimination of lenalidomide only occurs in the brain. It is acknowledged that the processes responsible for lenalidomide breakdown exist throughout the entire body, potentially varying in their activity dependent on the activity of the process in each tissue. If this non-renal elimination is caused by a spontaneous chemical reaction, then this process would be present in all tissues. While the proportion of renal to non-renal elimination in mice is unknown, in humans, 16% of lenalidomide clearance is attributed to non-renal sources of elimination when taken orally [25]. Assuming that the proportion of renal to non-renal elimination remains unchanged when administering lenalidomide intravenously, at least 7% of clearance is due to hydrolysis, but it is unclear if this is true for the mouse. This proportion of clearance was achieved when non-renal elimination was implemented in all tissues; however, this was with severe detriment to model predictions. Despite these flaws, they are only of importance when predicting lenalidomide metabolite concentrations, which are not expected to cause additional therapeutic activity [24].

The spleen is an important tissue for lenalidomide pharmacodynamics, as cancer cells can aggregate in this tissue during malignancy. While the models predict spleen

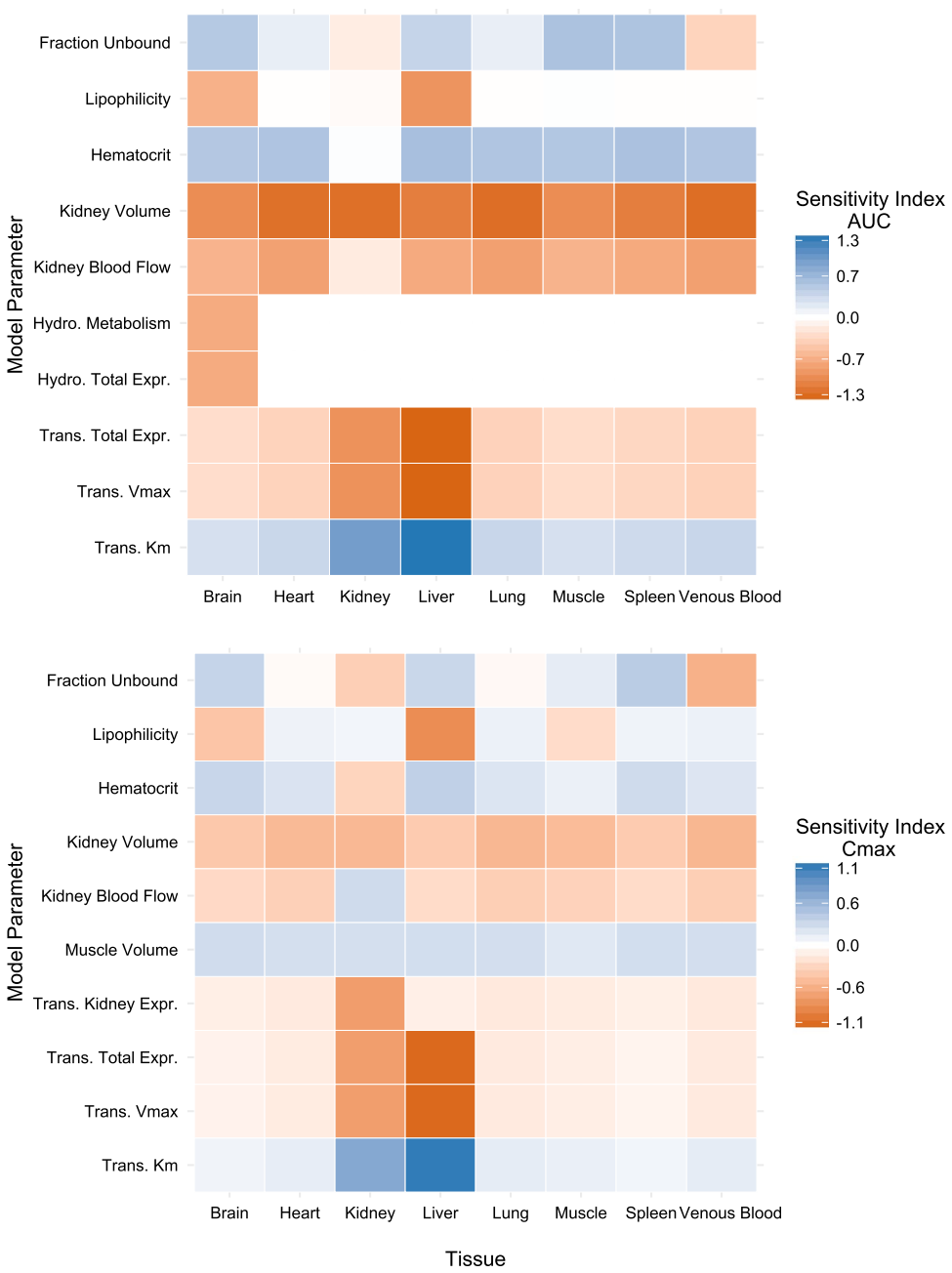

Fig. 5 Heat map of the local sensitivity analysis results for the final model using unspecified basolateral transporters in the brain compartment. It presents the sensitivity indices of pharmacokinetic metrics for the ten most sensitive parameters across all tissues. Sensitivity indices represent the relative change in the pharmacokinetic metric that results from changing parameter values. Upper panel shows sensitivity index values for the area under the concentration curve from time equals zero to infinity (AUC $_{0\text{-inf}}$) and the lower panel shows sensitivity index values for the maximum concentration (C_{max}). The intensity of the colour in each panel correlates with the magnitude of the parameter sensitivity, with blue representing a positive correlation between the parameter and the pharmacokinetic metric and red representing a negative correlation. Hydro. Metabolism and Hydro. Total Expr. refer to the non-renal elimination rate constant and total expression/presence of reactants, respectively. Trans. Total Expr. refers to the total expression of transporters, while Trans. Kidney Expr. refers to the expression of transporters in the kidney. Trans. V_{max} and Trans. Km refer to the parameters used in the Michaelis–Menten equation responsible for modelling transporter kinetics

concentrations relatively well, they fail to completely capture the distribution phase seen in the spleen tissue data, predicting that C_{max} is higher and occurs earlier than in the observed data. A more complex spleen model, differentiating between white pulp and red pulp, may improve these predictions and be useful in malignancies where spleen physiology changes, such as chronic lymphocytic leukaemia [45]. This would be an important extension of this work if the model was further developed to predict concentrations after an oral dose of lenalidomide. An oral lenalidomide model could be scaled using allometric theory to predict tissue concentrations in a human. Using such a model to predict tissue concentrations in humans may provide valuable insight into links between the tissue-specific pharmacokinetics and pharmacodynamics of lenalidomide while also providing insight into the utility of PBPK models for inter-species scaling for this class of compounds.

This is the first PBPK model to elucidate a detailed investigation of the physiological processes responsible for lenalidomide disposition in multiple tissues. While the model has been shown to accurately predict concentrations in tissues of importance to B-cell malignancies, it raises additional questions about the tissue pharmacokinetics of lenalidomide. If the physiology represented in PK-Sim® is correct, there are

clear unknowns regarding the drug's transport in and out of tissues. The transport of lenalidomide is important to its pharmacokinetics not only in the brain, but all tissues, where relevant transporters may be expressed. Being an analogue of thalidomide, the lenalidomide transporter(s) may be a nucleoside transporter, responsible for influx of the drug into the brain. Further experimentation into intestinal and brain transporters will remove this uncertainty of lenalidomide disposition throughout the body, giving a clearer explanation for the drug's tissue pharmacokinetics.

Acknowledgements The research produced was supported by an Australian Government Research Training Program Scholarship (to JHH). The authors acknowledge that the Australian Centre for Pharmacometrics is an initiative of the Australian Government as part of the National Collaborative Research Infrastructure Strategy. Additional support came from the National Institutes of Health (R01CA201382 to MAP) and an Eli Lilly Fellowship (to DMR).

Author contributions Participated in research design: JHH, RNU, SER, DMR, MAP, and DJRF. Conducted experiments: DMR. Contributed new reagents or analytical tools: RNU, MAP, and DJRF. Performed data analysis: JHH. Wrote or contributed to the writing of the manuscript: JHH, RNU, SER, DMR, MAP, and DJRF.

Compliance with ethical standards

Conflict of interest The authors declare that they have no conflict of interest.

References

1. Ghosh N, Grunwald MR, Fasan O, Bhutani M (2015) Expanding role of lenalidomide in hematologic malignancies. Cancer Manag Res 7:105–119. https://doi.org/10.2147/CMAR.S81310
2. Lopez-Girona A, Mendy D, Ito T, Miller K, Gandhi AK, Kang J, Karasawa S, Carmel G, Jackson P, Abbasian M, Mahmoudi A, Cathers B, Rychak E, Gaidarova S, Chen R, Schafer PH, Handa H, Daniel TO, Evans JF, Chopra R (2012) Cereblon is a direct protein target for immunomodulatory and antiproliferative activities of lenalidomide and pomalidomide. Leukemia 26(11):2326–2335. https://doi.org/10.1038/leu.2012.119
3. Zhu YX, Braggio E, Shi CX, Bruins LA, Schmidt JE, Van Wier S, Chang XB, Bjorklund CC, Fonseca R, Bergsagel PL, Orlowski RZ, Stewart AK (2011) Cereblon expression is required for the antimyeloma activity of lenalidomide and pomalidomide. Blood 118(18):4771–4779
4. Gandhi AK, Kang J, Havens CG, Conklin T, Ning Y, Wu L, Ito T, Ando H, Waldman MF, Thakurta A, Klippel A, Handa H, Daniel TO, Schafer PH, Chopra R (2014) Immunomodulatory agents lenalidomide and pomalidomide co-stimulate T cells by inducing degradation of T cell repressors Ikaros and Aiolos via modulation of the E3 ubiquitin ligase complex CRL4 (CRBN). Br J Haematol 164(1):811–821. https://doi.org/10.1111/bjh.12708
5. Zhu YX, Kortuem KM, Stewart AK (2013) Molecular mechanism of action of immune-modulatory drugs thalidomide, lenalidomide and pomalidomide in multiple myeloma. Leuk Lymphoma 54(4):683–687. https://doi.org/10.3109/10428194.2012.728597
6. Warren KE, Goldman S, Pollack IF, Fangusaro J, Schaiquevich P, Stewart CF, Wallace D, Blaney SM, Packer R, MacDonald T, Jakacki R, Boyett JM, Kun LE (2011) Phase I trial of lenalidomide in pediatric patients with recurrent, refractory, or progressive primary cns tumors: pediatric brain tumor consortium study PBTC-018. J Clin Oncol 29(3):324–329. https://doi.org/10.1200/JCO.2010.31.3601
7. Berg SL, Cairo MS, Russell H, Ayello J, Ingle AM, Lau H, Chen N, Adamson PC, Blaney SM (2011) Safety, pharmacokinetics, and immunomodulatory effects of lenalidomide in children and adolescents with relapsed/refractory solid tumors or myelodysplastic syndrome: a children's oncology group phase I consortium report. J Clin Oncol 29(3):316–323. https://doi.org/10.1200/JCO.2010.30.8387
8. Drappatz J, Wong ET, Schiff D, Kesari S, Batchelor TT, Doherty L, Lafrankie DC, Ramakrishna N, Weiss S, Smith ST, Ciampa A, Zimmerman J, Ostrowsky L, David K, Norden A, Barron L, Sceppa C, Black PM, Wen PY (2009) A pilot safety study of lenalidomide and radiotherapy for patients with newly diagnosed glioblastoma multiforme. Int J Radiat Oncol Biol Phys 73(1):222–227. https://doi.org/10.1016/j.ijrobp.2008.03.046
9. Fine HA, Kim L, Albert PS, Duic JP, Ma H, Zhang W, Tohnya T, Figg WD, Royce C (2007) A phase I trial of lenalidomide in patients with recurrent primary central nervous system tumors. Am Assoc Cancer Res 13(23):7101–7106. https://doi.org/10.1158/1078-0432.ccr-07-1546
10. Chanan-Khan A, Miller KC, Musial L, Lawrence D, Padmanabhan S, Takeshita K, Porter CW, Goodrich DW, Bernstein ZP, Wallace P, Spaner D, Mohr A, Byrne C, Hernandez-Ilizaliturri F, Chrystal C, Starostik P, Czuczman MS (2006) Clinical efficacy of lenalidomide in patients with relapsed or refractory chronic lymphocytic leukemia: results of a phase II study. J Clin Oncol 24(34):5343–5349. https://doi.org/10.1200/jco.2005.05.0401
11. Foucar K, McKenna RW, Frizzera G, Brunning RD (1982) Bone marrow and blood involvement by lymphoma in relationship to the lukes—collins classification. Cancer 49(5):888–897. https://doi.org/10.1002/1097-0142(19820301)49:5%3c888:AID-CNCR11%3e3.0.CO;2-K
12. Kyle RA, Gertz MA, Witzig TE, Lust JA, Lacy MQ, Dispenzieri A, Fonseca R, Rajkumar SV, Offord JR, Larson DR, Plevak ME, Therneau TM, Greipp PR (2003) Review of 1027 patients with newly diagnosed multiple myeloma. Mayo Clin Proc 78(1):21–33. https://doi.org/10.4065/78.1.21
13. Rozman C, Montserrat E (1995) Chronic lymphocytic leukemia. N Engl J Med 333(16):1052–1057. https://doi.org/10.1056/nejm199510193331606
14. Dankbar B, Padró T, Leo R, Feldmann B, Kropff M, Mesters RM, Serve H, Berdel WE, Kienast J (2000) Vascular endothelial growth factor and interleukin-6 in paracrine tumor-stromal cell interactions in multiple myeloma. Blood 95(8):2630–2636
15. Gupta D, Treon SP, Shima Y, Hideshima T, Podar K, Tai YT, Lin B, Lentzsch S, Davies FE, Chauhan D, Schlossman RL, Richardson P, Ralph P, Wu L, Payvandi F, Muller G, Stirling DI, Anderson KC (2001) Adherence of multiple myeloma cells to bone marrow stromal cells upregulates vascular endothelial growth factor secretion: therapeutic applications. Leukemia 15(12):1950–1961
16. Hideshima T, Chauhan D, Shima Y, Raje N, Davies FE, Tai YT, Treon SP, Lin B, Schlossman RL, Richardson P, Muller G, Stirling DI, Anderson KC (2000) Thalidomide and its analogs overcome drug resistance of human multiple myeloma cells to conventional therapy. Blood 96(9):2943–2950
17. Hofmeister CC, Yang X, Pichiorri F, Chen P, Rozewski DM, Johnson AJ, Lee S, Liu Z, Garr CL, Hade EM, Ji J, Schaaf LJ, Benson DM Jr, Kraut EH, Hicks WJ, Chan KK, Chen CS, Farag SS, Grever MR, Byrd JC, Phelps MA (2011) Phase I trial of lenalidomide and CCI-779 in patients with relapsed multiple myeloma: evidence for lenalidomide-CCI-779 interaction via

P-glycoprotein. J Clin Oncol 29(25):3427–3434. https://doi.org/10.1200/jco.2010.32.4962
18. Blum W, Klisovic RB, Becker H, Yang X, Rozewski DM, Phelps MA, Garzon R, Walker A, Chandler JC, Whitman SP, Curfman J, Liu S, Schaaf L, Mickle J, Kefauver C, Devine SM, Grever MR, Marcucci G, Byrd JC (2010) Dose escalation of lenalidomide in relapsed or refractory acute leukemias. J Clin Oncol 28(33):4919–4925. https://doi.org/10.1200/jco.2010.30.3339
19. Maddocks K, Ruppert AS, Browning R, Jones J, Flynn J, Kefauver C, Gao Y, Jiang Y, Rozewski DM, Poi M, Phelps MA, Harper E, Johnson AJ, Byrd JC, Andritsos LA (2014) A dose escalation feasibility study of lenalidomide for treatment of symptomatic, relapsed chronic lymphocytic leukemia. Leuk Res 38(9):1025–1029. https://doi.org/10.1016/j.leukres.2014.05.011
20. Maddocks K, Wei L, Rozewski D, Jiang Y, Zhao Y, Adusumilli M, Pierceall WE, Doykin C, Cardone MH, Jones JA, Flynn J, Andritsos LA, Grever MR, Byrd JC, Johnson AJ, Phelps MA, Blum KA (2015) Reduced occurrence of tumor flare with flavopiridol followed by combined flavopiridol and lenalidomide in patients with relapsed chronic lymphocytic leukemia (CLL). Am J Hematol 90(4):327–333. https://doi.org/10.1002/ajh.23946
21. Chen N, Ette E, Zhou S, Weiss D, Palmisano M (2013) Population pharmacokinetics and exposure-safety of lenalidomide in patients with multiple myeloma, myelodysplastic syndromes and mantle cell lymphoma. Blood 122(21):3234
22. Bridoux F, Chen N, Moreau S, Arnulf B, Moumas E, Abraham J, Desport E, Jaccard A, Fermand JP (2016) Pharmacokinetics, safety, and efficacy of lenalidomide plus dexamethasone in patients with multiple myeloma and renal impairment. Cancer Chemother Pharmacol 78(1):173–182. https://doi.org/10.1007/s00280-016-3068-9
23. Corporation C (2017) Product monograph: revlimid® lenalidomide capsules. https://media.celgene.com/content/uploads/sites/23/Revlimid-Product_Monograph_-_English_Version.pdf. Accessed 6 Mar 2017
24. Chen N, Wen L, Lau H, Surapaneni S, Kumar G (2012) Pharmacokinetics, metabolism and excretion of [(14)C]-lenalidomide following oral administration in healthy male subjects. Cancer Chemother Pharmacol 69(3):789–797. https://doi.org/10.1007/s00280-011-1760-3
25. Chen N, Lau H, Kong L, Kumar G, Zeldis JB, Knight R, Laskin OL (2007) Pharmacokinetics of lenalidomide in subjects with various degrees of renal impairment and in subjects on hemodialysis. J Clin Pharmacol 47(12):1466–1475. https://doi.org/10.1177/0091270007309563
26. Tong Z, Yerramilli U, Surapaneni S, Kumar G (2014) The interactions of lenalidomide with human uptake and efflux transporters and UDP-glucuronosyltransferase 1A1: lack of potential for drug–drug interactions. Cancer Chemother Pharmacol 73(4):869–874. https://doi.org/10.1007/s00280-014-2415-y
27. Kumar G, Lau H, Laskin O (2009) Lenalidomide: in vitro evaluation of the metabolism and assessment of cytochrome P450 inhibition and induction. Cancer Chemother Pharmacol 63(6):1171–1175. https://doi.org/10.1007/s00280-008-0867-7
28. Connarn JN, Hwang R, Gao Y, Palmisano M, Chen N (2017) Population pharmacokinetics of lenalidomide in healthy volunteers and patients with hematologic malignancies. Clin Pharmacol Drug Dev 7(5):465–473. https://doi.org/10.1002/cpdd.372
29. Guglieri-López B, Pérez-Pitarch A, Moes DJAR, Porta-Oltra B, Climente-Martí M, Guchelaar HJ, Merino-Sanjuán M (2017) Population pharmacokinetics of lenalidomide in multiple myeloma patients. Cancer Chemother Pharmacol 79(1):189–200. https://doi.org/10.1007/s00280-016-3228-y
30. Anwer S, Collings F, Trace K, Sun Y, Sternberg A (2013) Cerebrospinal fluid penetrance of lenalidomide in meningeal myeloma. Br J Haematol 162(2):281–282. https://doi.org/10.1111/bjh.12351
31. Muscal JA, Sun Y, Nuchtern JG, Dauser RC, McGuffey LH, Gibson BW, Berg SL (2012) Plasma and cerebrospinal fluid pharmacokinetics of thalidomide and lenalidomide in nonhuman primates. Cancer Chemother Pharmacol 69(4):943–947. https://doi.org/10.1007/s00280-011-1781-y
32. Rozewski DM, Herman SEM, Towns WH, Mahoney E, Stefanovski MR, Shin JD, Yang X, Gao Y, Li X, Jarjoura D, Byrd JC, Johnson AJ, Phelps MA (2012) Pharmacokinetics and tissue disposition of lenalidomide in mice. AAPS J 14(4):872–882. https://doi.org/10.1208/s12248-012-9401-2
33. Upton RN, Foster DJR, Abuhelwa AY (2016) An introduction to physiologically-based pharmacokinetic models. Pediatr Anesth 26(11):1036–1046. https://doi.org/10.1111/pan.12995
34. Liu Q, Farley KL, Johnson AJ, Muthusamy N, Hofmeister CC, Blum KA, Schaaf LJ, Grever MR, Byrd JC, Dalton JT, Phelps MA (2008) Development and validation of a highly sensitive liquid chromatography/mass spectrometry method for simultaneous quantification of lenalidomide and flavopiridol in human plasma. Ther Drug Monit 30(5):620–627. https://doi.org/10.1097/FTD.0b013e318185813d
35. Eissing T, Kuepfer L, Becker C, Block M, Coboeken K, Gaub T, Goerlitz L, Jaeger J, Loosen R, Ludewig B, Meyer M, Niederalt C, Sevestre M, Siegmund H-U, Solodenko J, Thelen K, Telle U, Weiss W, Wendl T, Willmann S, Lippert J (2011) A computational systems biology software platform for multiscale modeling and simulation: integrating whole-body physiology, Disease biology, and molecular reaction networks. Front Physiol 2:4. https://doi.org/10.3389/fphys.2011.00004
36. Beal SL (2001) Ways to fit a PK model with some data below the quantification limit. J Pharmacokinet Pharmacodyn 28(5):481–504. https://doi.org/10.1023/A:1012299115260
37. RC Team (2017) R: a language and environment for statistical computing. R Foundation for Statistical Computing, Vienna
38. Wishart DS, Feunang YD, Guo AC, Lo EJ, Marcu A, Grant JR, Sajed T, Johnson D, Li C, Sayeeda Z, Assempour N, Iynkkaran I, Liu Y, Maciejewski A, Gale N, Wilson A, Chin L, Cummings R, Le D, Pon A, Knox C, Wilson M (2018) DrugBank 5.0: a major update to the DrugBank database for 2018. Nucleic Acids Res 46(D1):D1074–D1082. https://doi.org/10.1093/nar/gkx1037
39. DrugBank (2017) Lenalidomide. https://www.drugbank.ca/drugs/DB00480. Accessed 12 Sept 2017
40. Yue F, Cheng Y, Breschi A, Vierstra J, Wu W, Ryba T, Sandstrom R, Ma Z, Davis C, Pope BD, Shen Y, Pervouchine DD, Djebali S, Thurman RE, Kaul R, Rynes E, Kirilusha A, Marinov GK, Williams BA, Trout D, Amrhein H, Fisher-Aylor K, Antoshechkin I, DeSalvo G, See LH, Fastuca M, Drenkow J, Zaleski C, Dobin A, Prieto P, Lagarde J, Bussotti G, Tanzer A, Denas O, Li K, Bender MA, Zhang M, Byron R, Groudine MT, McCleary D, Pham L, Ye Z, Kuan S, Edsall L, Wu YC, Rasmussen MD, Bansal MS, Kellis M, Keller CA, Morrissey CS, Mishra T, Jain D, Dogan N, Harris RS, Cayting P, Kawli T, Boyle AP, Euskirchen G, Kundaje A, Lin S, Lin Y, Jansen C, Malladi VS, Cline MS, Erickson DT, Kirkup VM, Learned K, Sloan CA, Rosenbloom KR, Lacerda de Sousa B, Beal K, Pignatelli M, Flicek P, Lian J, Kahveci T, Lee D, Kent WJ, Ramalho Santos M, Herrero J, Notredame C, Johnson A, Vong S, Lee K, Bates D, Neri F, Diegel M, Canfield T, Sabo PJ, Wilken MS, Reh TA, Giste E, Shafer A, Kutyavin T, Haugen E, Dunn D, Reynolds AP, Neph S, Humbert R, Hansen RS, De Bruijn M, Selleri L, Rudensky A, Josefowicz S, Samstein R, Eichler EE, Orkin SH, Levasseur D, Papayannopoulou T, Chang KH, Skoultchi A, Gosh S, Disteche C, Treuting P, Wang Y, Weiss MJ, Blobel GA, Cao X, Zhong S, Wang T, Good PJ, Lowdon RF, Adams LB, Zhou XQ, Pazin MJ, Feingold EA, Wold B, Taylor J, Mortazavi A, Weissman SM, Stamatoyannopoulos JA, Snyder MP, Guigo R, Gingeras TR, Gilbert DM, Hardison RC, Beer MA, Ren B (2014) A comparative encyclopedia of DNA

elements in the mouse genome. Nature 515(7527):355–364. https://doi.org/10.1038/nature13992
41. Ferguson CS, Tyndale RF (2011) Cytochromes P450 in the brain: emerging evidence for biological significance. Trends Pharmacol Sci 32(12):708–714. https://doi.org/10.1016/j.tips.2011.08.005
42. Zhou S, Li Y, Kestell P, Schafer P, Chan E, Paxton JW (2005) Transport of thalidomide by the human intestinal caco-2 monolayers. Eur J Drug Metab Pharmacokinet 30(1–2):49–61
43. Ball K, Bouzom F, Scherrmann J-M, Walther B, Declèves X (2013) Physiologically based pharmacokinetic modelling of drug penetration across the blood-brain barrier–towards a mechanistic IVIVE-based approach. AAPS J 15(4):913–932. https://doi.org/10.1208/s12248-013-9496-0
44. Chowdhury G, Shibata N, Yamazaki H, Guengerich FP (2014) Human cytochrome P450 oxidation of 5-hydroxythalidomide and pomalidomide, an amino analog of thalidomide. Chem Res Toxicol 27(1):147–156. https://doi.org/10.1021/tx4004215
45. Lampert I, Catovsky D, Marsh GW, Child JA, Galton DAG (1980) The histopathology of prolymphocytic leukaemia with particular reference to the spleen: a comparison with chronic lymphocytic leukaemia. Histopathology 4(1):3–19. https://doi.org/10.1111/j.1365-2559.1980.tb02893.x
46. Willmann S, Lippert J, Schmitt W (2005) From physicochemistry to absorption and distribution: predictive mechanistic modelling and computational tools. Expert Opin Drug Metab Toxicol 1(1):159–168. https://doi.org/10.1517/17425255.1.1.159